A. Brömme, C. Busch, A. Dantcheva, C. Rathgeb and A. Uhl (Eds.): BIOSIG 2018,
Lecture Notes in Informatics (LNI), Gesellschaft für Informatik, Bonn 2018 1

Fingerprint Presentation Attack Detection using Laser Speckle Contrast Imaging

Pascal Keilbach[1], Jascha Kolberg[2], Marta Gomez-Barrero[2], Christoph Busch[2],
Hanno Langweg[1]

Abstract: With the increased deployment of biometric authentication systems, some security concerns have also arisen. In particular, presentation attacks directed to the capture device pose a severe threat. In order to prevent them, liveness features such as the blood flow can be utilised to develop presentation attack detection (PAD) mechanisms. In this context, laser speckle contrast imaging (LSCI) is a technology widely used in biomedical applications in order to visualise blood flow. We therefore propose a fingerprint PAD method based on textural information extracted from preprocessed LSCI images. Subsequently, a support vector machine is used for classification. In the experiments conducted on a database comprising 32 different artefacts, the results show that the proposed approach classifies correctly all bona fides. However, the LSCI technology experiences difficulties with thin and transparent overlay attacks.

Keywords: Presentation Attack Detection, Laser Speckle Contrast Imaging, LSCI, Fingerprint

1 Introduction

The use of biometrics has been increasing over the last few years due to its efficency, reliability and convenience [JRN11]. As any other authentication technology, biometric systems are also vulnerable to external attacks. In particular, an attacker may not require further knowledge about the biometric system to deceive it. Instead, he may conduct a presentation attack (PA) by simply presenting to the biometric capture device a presentation attack instrument (PAI), such as an artificial finger made of rubber or a fingerprint overlay. Hence, to ensure the integrity of the authentication process, automatic presentation attack detection (PAD) becomes crucial. All these facts have led to an increased interest on this research topic: public institutions have launched and funded several projects, such as BEAT [BE12] or ODIN [OI16], and the standardisation efforts have led to the development of the ISO/IEC IS 30107 on biometric presentation attack detection [IS16].

In this context, PAD methods have been proposed in the last decade for several biometric characteristics, including iris [GGB17], fingerprint [SB14], or face [GMF14]. For fingerprints, Hengfoss *et al.* analysed extensively the multi-spectral signatures of the living against cadaver fingers using spectroscopy techniques [He11]. More recently, three methods based on pulse, pressure, and illumination with different wavelengths were presented

[1] Department of Computer Science, Hochschule Konstanz, Germany, {pascal.keilbach, hanno.langweg}@htwg-konstanz.de

[2] da/sec - Biometrics and Internet Security Research Group, Hochschule Darmstadt, Germany, {jascha.kolberg, marta.gomez-barrero, christoph.busch}@h-da.de

in [Dr13], where 2% of the bona fide samples and 10% PA samples are miss-classified. Furthermore, the authors noted that some skin diseases have a negative influence on PAD based on liveness measurements.

Other fingerprint PAD approaches build upon conventional capture devices. However, as any other pattern recognition task, PAD can benefit from complementary sources of information. For instance, laser speckle contrast imaging (LSCI) is typically used in biomedical applications as a tool for imaging and monitoring microvascular blood flow in different kinds of biological tissues, such as skin and retina, or in neuroscience [Va16, Se13]. Therefore, it can be useful for PAD purposes, in order to measure whether there is blood flow in the presented characteristic.

Within the biometrics community, however, LSCI is not yet widely used. Among the very few examples, retinal scanning based on LSCI data is proposed in [SC16]. The retinal LSCI images provide a blood flow profile, which is compared to the vasculature pattern of the retina. If the regions of flow match the retinal vasculature pattern, the sample is classified as bona fide. However, no PAs were considered in [SC16].

This work presents, to the best of our knowledge, the first approach to use LSCI for fingerprint PAD. A sensor to acquire the laser speckle images from the finger is described, which has been designed within the ODIN program [OI16]. We then present the implementation of the corresponding pre-processing techniques to extract the LSCI images. Textural information is subsequently extracted from the LSCI images, and classification is carried out with support vector machines (SVMs). Therefore, the proposed technique is efficient and can be implemented on real time applications. In addition, two fusion schemes for the different features extracted have been analysed. We have tested a collection of 32 different PAI species, including both complete thick fake fingers and more challenging overlays. Most of the PAIs were correctly detected.

The rest of the paper is organised as follows. Sect. 2 explains the core concepts of LSCI. The proposed PAD method is described in Sect. 3. Sect. 4 summarises the experimental evaluation carried out and final conclusions are drawn in Sect. 5.

2 Laser Speckle Contrast Imaging (LSCI)

When coherent light (i.e. laser light) is reflected by a sufficiently rough surface, the light is scattered, and a granular pattern of dark and bright spots occurs. This is called a speckle pattern, which results from a random interference pattern: the scattered coherent light waves either add up, resulting in bright spots, or cancel out, resulting in dark spots [Se13]. For many laser applications, this effect is considered noise, and various techniques were developed to reduce the laser speckle effect [Va16].

It was Goodman who attempted to statistically quantify the speckle effects [Go75]. This allowed the measurement of, for instance, surface roughness or surface temperature [Pe92]. Furthermore, laser light has a certain penetration depth, and if moving scatterers are present (i.e. blood) the speckle pattern will change over time [Va16]. Therefore, speckle patterns

can be used to characterise motion of objects or relative flow of particles in a medium [DK08].

If the aforementioned patterns are captured with a camera, the term laser speckle contrast imaging (LSCI) [Va16] is used. Depending on the degree of motion and camera parameters like exposure time, moving areas will appear blurred in the laser speckle image. The degree of blurring is called speckle contrast and is also one of the major characteristics of the laser speckle phenomenon. Goodman showed that, in perfect conditions, the standard deviation of the speckle pattern is equal to its mean intensity [Go75]. Following this idea, the speckle contrast K is defined as the ratio between the standard deviation (σ) and the mean intensity ($\langle I \rangle$):

$$K = \frac{\sigma}{\langle I \rangle} \tag{1}$$

The contrasting neighbourhood can be analysed either in the spatial (K_s) or in the temporal (K_t) domain. To calculate the spatial speckle contrast, a window (e.g., of size 3×3) iterates over the laser speckle images and calculates the contrast for each pixel. The temporal approach uses multiple laser speckle images to see how a single pixel changes over time. It is important to note that temporal contrast reduces temporal resolution, while spatial contrast reduces spatial resolution. Therefore, the best approach depends on the application context (i.e., which dimension is more important to preserve) [Va16].

3 Presentation Attack Detection Method

Our PAD approach based on LSCI consists of three basic steps: pre-processing, feature extraction, and classification. Each step is described in the following sections.

3.1 Image Acquisition and Pre-Processing

The finger LSCI sensor was developed within the BATL project [BA17] of the ODIN program [OI16], in conjunction with our partners at TREX Enterprises and the University of South California. In particular, a Hamamatsu InGaAs area image sensor G11097-0606S, which operates at a wavelength of 1310 nm at an exposure time of 1 ms, is used to capture the LSCI data. This setup delivers 1000 laser speckle images per second, each of size 64×64 pixels. The laser used to illuminate the finger samples is an Eblana Photonics EP1310-ADF-B laser diode.

As mentioned above, the images delivered have a resolution of only 64×64 pixels. Therefore, it is more important to preserve the spatial resolution, and accept a loss of temporal resolution. After an exhaustive analysis of both spatial and temporal contrast calculation methods [BD10, Se13, SC16, Va16], the temporal approach with a neighbourhood of 25 consecutive laser speckle images was chosen. It is important to note that in the temporal

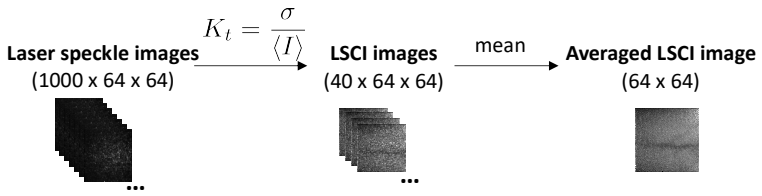

Fig. 1: Pre-processing to obtain a LSCI image out of a stack of 1000 laser speckle images. The averaged LSCI image is the basis for the subsequent steps, i.e. feature extraction and classification.

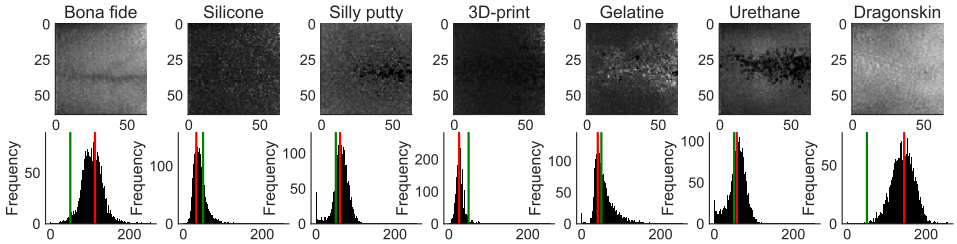

Fig. 2: Examples of averaged LSCI images of bona fide and PA samples. The corresponding greyscale histograms are shown in the second row, where the red vertical line represents the highest peak and the green line the pre-selection decision threshold (see Sect. 3.4).

domain, if no motion is present, the pixel will appear with approximately the same intensity along several images, leading to a low σ, and therefore a low K_t (see Eq. 1). On the other hand, if motion is present, the same pixel will appear with different intensities along several images, leading to high σ, and therefore a high K_t [Va16].

As illustrated in Fig. 1, LSCI images are calculated over the selected temporal neighbourhood of 25 consecutive laser speckle images from the initial 1000 laser speckle images, thus resulting in 40 LSCI images. In order to put all the information in a single LSCI image, the next step is to average the intermediate 40 LSCI images into a single one. Fig. 2 shows a selection of averaged LSCI images of a bona fide and several PAIs.

3.2 Feature Extraction

As explained in Sect. 2, for the temporal LSCI calculation, a low K_t indicates no motion, whereas a high K_t indicates motion, and hence blood flow. Thus, greyscale values of the averaged LSCI images are a direct representation of motion. This is shown in Fig. 2, where PAIs yield darker LSCI images and thus histograms with heavier left tails, whereas the bona fide sample produces a brighter LSCI image and a heavier right tail in the histogram.

In addition to greyscale values, a deeper analysis of the averaged LSCI images of Fig. 2 reveals texture information in them. Whereas bona fide samples have a smooth texture, which stems from the biological tissue, materials like silicone, silly putty, or urethane have a rough and stained texture.

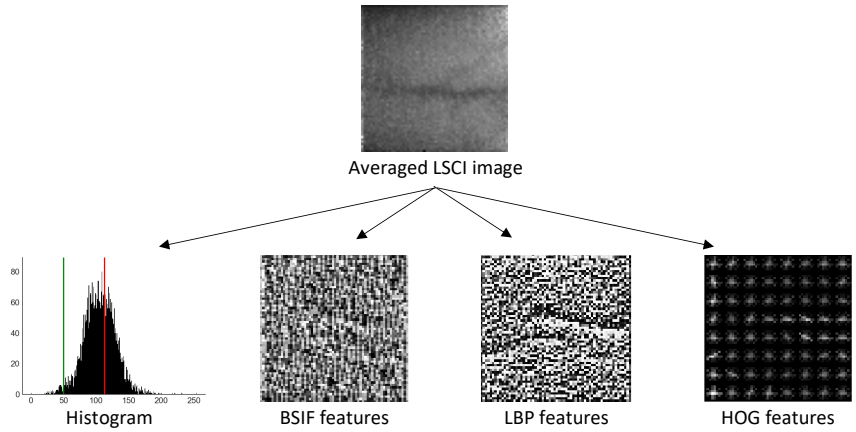

Fig. 3: Features extracted from each averaged LSCI image, namely: *i*) greyscale histogram, *ii*) BSIF, *iii*) HOG, *iv*) and LBP descriptors.

Taking both facts into account, both greyscale and texture information will be extracted from the LSCI images, as it is depicted in Fig. 3. The former will be represented with 256-bin histograms. On the other hand, the well-known Local Binary Pattern (LBP) and Binarized Statistical Image Features (BSIF) texture descriptors [FWW15] have been chosen, since they have showed a higher performance in comparative evaluations [Gh17] with respect to other measures. Finally, based in the observation that veins are only present in bona fide samples, as a contrasted line with no pre-defined shape but an approximately horizontal direction, these will be detected with the Histogram of Oriented Gradients (HOG) descriptor [FWW15].

3.3 Single Classification

Being PAD a binary decision between the bona fide (class 0) and PA (class 1) classes, SVMs are an appropriate choice for a classifier [St17]. For each feature descriptor (i.e., histogram, LBP, HOG, BSIF), a separate SVM was trained and tested.

In addition, the sensor captures three LSCI images per sample (see Fig. 4). This allows us to implement a more robust PAD method, since the final decision relies on the three LSCI images. In particular, for each of the three LSCI images of a given sample, the SVM returns the estimated class r_i with $i = 1,2,3$, as indicated in Fig. 4. Subsequently, the final decision for the given sample is reached by a majority voting of the result tuple:

$$r_{\text{sample}} = \text{majority}\,(r_1, r_2, r_3) \tag{2}$$

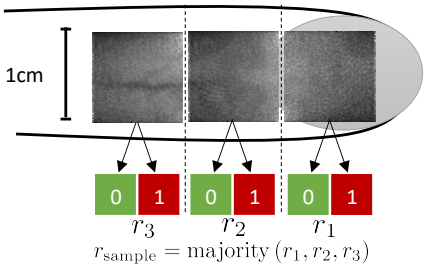

Fig. 4: Data acquisition for a single finger sample, where 3 LSCI images are captured. The individual decisions r_i for each image are fused with a majority vote rule: $r_{\text{sample}} = \text{majority}\,(r_1, r_2, r_3)$.

3.4 Fused Classification

In order to fuse the information yielded by each extracted feature described in Sect. 3.2, two different approaches have been considered, as shown in Fig. 5. In both cases, and in order to filter obvious PAs, a pre-selection PAD based on the following observation is carried out: the greyscale histograms of the LSCI images in Fig. 2 show an obvious peak bin (highlighted with a red vertical line), located at different positions for bona fides and PAs. Therefore, we will compare the peak bin of the histogram against a threshold (shown in green): if it is lower than the threshold, the samples is classified as PA, and otherwise further processing will start. In order to avoid a misclassification of bona fide samples, we recommend a low threshold such as the one depicted in green in Fig. 2.

After the pre-selection step, the **cascade PAD** (Fig. 5a) focuses on time efficiency. After each feature extraction process, ordered from the simplest to the most complex, a decision can be made: if the sample is classified as PA, that is the final decision. Otherwise, the next feature extraction algorithm is executed.

Another alternative is to predict the class by the **majority** of the single results, as shown in Fig. 5b. In this case, if no PA was detected at pre-selection, the sample is subsequently tested against the remaining PAD features. The final result is determined by the majority of these individual single results (i.e., histogram, LBP and HOG).

4 Experimental Evaluation

4.1 Dataset and Experimental Setup

The dataset was acquired at the University of South California within the BATL project [BA17] of the ODIN program [OI16]. It comprises 545 bona fide samples and 225 PA samples, stemming from 32 different PAIs (e.g., overlays fabricated with dragonskin, latex, school glue, or urethane, thick fingers made with several colours of play doh and wax or 3D prints, and the corresponding variations coated with conductive paint). Bona fide samples were captured from all five fingers of the right hand from 163 participants, and PAIs were

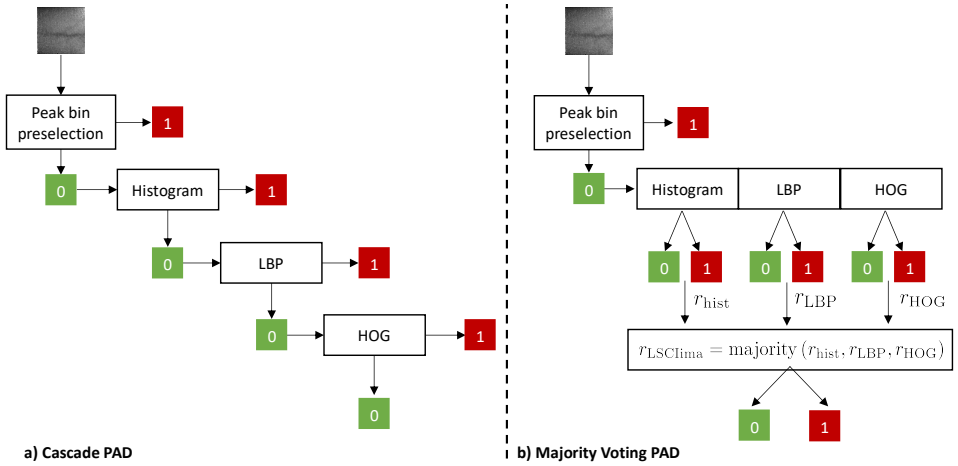

Fig. 5: Fused PAD methods, based on (a) a cascade decision and (b) an initial pre-selection based on the histogram features and a majority voting of the remaining features.

	# Samples	# Attack samples	# Bona fide samples
Training set	136	70 (51%)	66 (49%)
Test set	634	155 (24%)	479 (76%)

Tab. 1: Partition of training and test data.

also applied to all fingers. Subsequently, the data was manually checked and bad quality samples (i.e., due to finger motion) were excluded.

For each of the total 770 samples, laser speckle images were acquired from three contiguous areas, moving from the fingertip leftwards (see Fig. 4), thus resulting in a total of $770 \cdot 3 = 2310$ LSCI images. The data was split into disjoint training and test sets as shown in Table 1, using a similar number of each class for training to avoid bias towards one class. In a first step, cross validation was conducted to find the best parameters for the SVM. It should be also noted that, in order to establish a fair benchmark of the results, the same training and test data were used for each SVM.

The test results are evaluated in compliance with the ISO/IEC 30107-3 on Biometric presentation attack detection - testing and reporting [IS17]. To that end, the following metrics are used: i) Attack Presentation Classification Error Rate (APCER), or percentage of attack presentations wrongly classified as bona fide presentations; and ii) Bona Fide Presentation Classification Error Rate (BPCER), or percentage of bona fide presentations wrongly classified as presentation attacks.

	Histogram	LBP	HOG	BSIF	Pre-selection	Cascade	Majority Vote
APCER (%)	30.97	16.77	12.90	18.06	27.10	10.97	15.48
BPCER (%)	0.21	0.42	0.63	2.71	0.21	0.84	0.21

Tab. 2: Test results of the implemented PAD methods.

4.2 Results and Discussion

The test results for each of the feature descriptors (i.e., histogram, LBP, HOG, BSIF) are presented in Table 2. As it may be observed, the histogram features achieve the lowest BPCER (0.21%). However, they yield the highest APCER (30.97%). On the other hand, the more complex texture descriptors achieve a better balance between both error rates: while LBP and HOG have a similarly low BPCER (0.42% and 0.63%), they achieve a much lower APCER (16.77% and 12.90%) than the histogram features. Finally, BSIF performs worse than the last two descriptors (BPCER = 2.71% and APCER = 18.06%). Hence, BSIF is excluded from the fused approaches described in Sect. 3.4 and Fig. 5.

A deeper analysis of the APCEs shows that most of them stem from thin and transparent overlays (i.e. dragonskin). In more detail, the percentage of APCEs derived from these overlays ranges from 77% for the histogram features to 96% for LBP. The reason behind these errors lies on the fact that LSCI analyses the blood flow, and this is still visible through these overlays (see Fig. 2).

In order to further improve the results, we have also considered the fused PAD described in Sect 3.4. The results of these fused methods are also shown in Table 2. As it may be observed, the cascade PAD reduces the APCER, because PAs are filtered in each step, and only a PA that passes all single PAD methods will be wrongly classified as a bona fide. From the same reasoning follows an increase on the BPCER until 0.84%. On the other hand, the majority voting PAD provides a low and robust BPCER of 0.21%, which is equivalent to one error in the test set. Furthermore, an analysis of the LSCI images of this misclassified sample shows that it is of poor quality, most probably caused by a failure in the capturing process. Finally, with an APCER of 15.48%, the APCER of the majority PAD is not as low as with cascade PAD, but the second lowest of the combined PAD methods.

5 Conclusion

We have proposed a PAD approach for fingerprints based on LSCI, a technology capable of visualising blood flow. Four different types of features (i.e., histograms, LBP, HOG, and BSIF) are extracted from the LSCI images and classified with SVMs. In addition to the individual decisions for each feature set, we have analysed two different fusion schemes in order to achieve a more robust PAD method.

Our experiments on a database comprising 32 different PAIs show that LSCI achieves remarkable results for PAD purposes. In particular, the majority voting fusion achieves a

BPCER as low as 0.21%, which is equivalent to one misclassified bona fide presentation. At the same time, an APCER of 15.48% shows the main limitation of LSCI for PAD purposes: it is not capable of detecting thin and transparent overlays, like dragonskin.

Our future work will focus on a rigorous analysis of machine learning techniques, in order to find the best classifier or SVM parameters, and a larger database collection. Furthermore, besides greyscale and texture information, motion descriptors will be researched, since LSCI contains motion information.

Acknowledgements

This research is based upon work supported in part by the Office of the Director of National Intelligence (ODNI), Intelligence Advanced Research Projects Activity (IARPA) under contract number 2017-17020200005. The views and conclusions contained herein are those of the authors and should not be interpreted as necessarily representing the official policies, either expressed or implied, of ODNI, IARPA, or the U.S. Government. The U.S. Government is authorized to reproduce and distribute reprints for governmental purposes notwithstanding any copyright annotation therein.

This work was partially supported by the German Federal Ministry of Education and Research (BMBF) as well as by the Hessen State Ministry for Higher Education, Research and the Arts (HMWK) within the Center for Research in Security and Privacy (CRISP, `www.crisp-da.de`). This research was carried out during an internship of P. Keilbach at da/sec.

References

[BA17] BATL: , Biometric Authentication with a Timeless Learner, 2017.

[BD10] Boas, D.; Dunn, A.: Laser Speckle Contrast Imaging in Biomedical Optics. Journal of Biomedical Optics, 15(1):011109, 2010.

[BE12] BEAT: , Biometrics Evaluation and Testing, 2012. `http://www.beat-eu.org/`.

[DK08] Duncan, D.; Kirkpatrick, S.: Can Laser Speckle Flowmetry be made a Quantitative Tool? Journal of the Optical Society of America, 25(8):2088, 2008.

[Dr13] Drahansky, M.; Dolezel, M.; Michal, J.; Brezinova, E.; Yim, J. et al.: New Optical Methods for Liveness Detection on Fingers. BioMed Research International, 2013:197925, 2013.

[FWW15] Fan, B.; Wang, Z.; Wu, F.: Local Image Descriptor: Modern Approaches. Springer, 2015.

[GGB17] Galbally, J.; Gomez-Barrero, M.: Presentation Attack Detection in Iris Recognition. In (Rathgeb, Christian Rathgeb; Busch, Christoph Busch, eds): Iris and Periocular Biometric Recognition, pp. 235–263. Institution of Engineering and Technology, 2017.

[Gh17] Ghiani, L.; Yambay, D. A.; Mura, V.; Marcialis, G. L.; Roli, F.; Schuckers, S.: Review of the Fingerprint Liveness Detection (LivDet) Competition Series: 2009 to 2015. Image and Vision Computing, 58:110–128, 2017.

[GMF14] Galbally, J.; Marcel, S.; Fierrez, J.: Biometric Antispoofing Methods: A Survey in Face Recognition. IEEE Access, 2:1530–1552, 2014.

[Go75] Goodman, J. W.: Statistical Properties of Laser Speckle Patterns. In (Dainty, J. C., ed.): Laser Speckle and Related Phenomena, volume 9, pp. 9–75. Springer, 1975.

[He11] Hengfoss, C.; Kulcke, A.; Mull, G.; Edler, C.; Püschel, K.; Jopp, E.: Dynamic Liveness and Forgeries Detection of the Finger Surface on the Basis of Spectroscopy in the 400–1650nm Region. Forensic Science International, 212(1):61–68, 2011.

[IS16] ISO/IEC JTC1 SC37 Biometrics: . ISO/IEC 30107-1. Information Technology - Biometric presentation attack detection - Part 1: Framework. International Organization for Standardization, 2016.

[IS17] ISO/IEC JTC1 SC37 Biometrics: . ISO/IEC IS 30107-3. Information Technology - Biometric presentation attack detection - Part 3: Testing and Reporting. ISO, 2017.

[JRN11] Jain, A.; Ross, A.; Nandakumar, K.: Introduction to Biometrics. Springer, 2011.

[OI16] ODNI; IARPA: , IARPA-BAA-16-04 (Thor), 2016. `https://www.iarpa.gov/index.php/research-programs/odin/odin-baa`.

[Pe92] Persson, U.: Real Time Measurement of Surface Roughness on Ground Surfaces Using Speckle-contrast Technique. Optics and Lasers in Engineering, 17(2):61–67, 1992.

[SB14] Sousedik, C.; Busch, C.: Presentation Attack Detection Methods for Fingerprint Recognition Systems: A Survey. IET Biometrics, 3(4):219–233, 2014.

[SC16] Shaydyuk, N.; Cleland, T.: Biometric Identification via Retina Scanning with Liveness Detection Using Speckle Contrast Imaging. In: Proc. ICCST. 2016.

[Se13] Senarathna, J.; Rege, A.; Li, N.; Thakor, N. V.: Laser Speckle Contrast Imaging: Theory, Instrumentation and Applications. IEEE Reviews in Biomedical Engineering, 6:99–110, 2013.

[St17] Stamp, M.: Introduction to Machine Learning with Applications in Information Security. CRC Press, London, 1st ed. edition, 2017.

[Va16] Vaz, P.; Humeau-Heurtier, A.; Figueiras, E.; Correia, C.; Cardoso, J.: Laser Speckle Imaging to Monitor Microvascular Blood Flow: A Review. IEEE Reviews in Biomedical Engineering, 9:106–120, 2016.